Hawassa University Journals - Ethiopia
Ethiopian Journal of Engineering and Technology (EJET)
Volume – 1, 2022, Pages 29–41. https://doi.org/10.82127/fgbnht38

Design and Development of Nanomaterial Based Digital Electronic Thermometer Probe: From Material-Device

Almaw Ayele Aniley

School of Electrical and Computer Engineering, Debre Markos University, Debre Markos, Ethiopia. E-Mail: lingerayele@gmail.com

Abstract

Temperature is defined as the measure of the average kinetic energy of the particles in materials. It is a fundamental quantity which affects any object and process including industrial processes, electrical systems' components, life and health of living things, agricultural soil, highways, buildings, dams, environment, etc. So, it should be properly quantified and controlled using highly accurate, precise, environmentally friendly, in-situ, low-power and inexpensive thermometers. There are many kinds of thermometers with the disadvantages of high power requirement, possession of poison sensing materials, high cost, inaccurate and imprecise. Here, we discuss the development of nanoceramic nickel manganate ($NiMn_2O_4$) thermistor powder based digital electronic thermometer probe. The nanomaterial was synthesized using acetates of Nickel (Ni) and Manganese (Mn) as precursor materials by using the solution route technique. The fabricated powder was characterized using field emission scanning electronic microscopy (FeSEM) and energy dispersive spectroscopy (EDS) for its morphology and composition respectively. Powder x-ray diffraction (XRD) was also used to determine the crystal structure and crystallite size of the sample. The sample is unformed in morphology, spinel in structure, 24 nm in average crystallite size and composed of Ni, Mn and O_2 in the proper ratio. The 0.35 gm of the powder was filled and pressed well in 2 mm diameter and 2 cm long cylindrical tube to fabricate and characterize the thermistor based thermometer. The resulting thermistor was characterized and calibrated using the Stein and Hart and the β-coefficient thermistor models. The embedded system for the thermometer was developed using atmega328 microprocessor-based microcontroller, a simple voltage divider electric circuit, stainless steel cylindrical tube and 3D printed package. The system was programmed using Arduino programming integrated development environment (Arduino IDE). The features of resulting thermometer are 4-digit precision, 0 ℃-70 ℃ range of temperature measurement, 5 V DC power supply requirement, contains environmental friendly chemicals and is highly accurate. It can be used primarily in agriculture. It can also be used in industry, medicine, automobile, environment, food processing, home automation, etc. Additionally, it can be the element of sensor nodes in wireless sensor networks (WSNs) and Internet of Things (IoT) technology in automation.

Keywords: Thermometer probe, nanoceramic, $NiMn_2O_4$, Digital, Temperature

1. Introduction

A thermometer is an instrument used to measure temperature. It is used in industry, medicine(Husain et al., 2014; Ota et al., 2017; Sun et al., 2018), agriculture(Almaw Ayele Aniley et al., A 2017; Almaw Ayele Aniley et al., 2019; Almaw Ayele Aniley et al., 2019; Naveen Kumar S K et al., 2019), home automation(David et al. 2015; Hamed and Hamed 2015; Reza et al., 2018), food processing, environment, and research(Goswami and Kumar, 2018; Priyadarshi, 2015; Sahu et al., 2015). World metrological organization (WMO) defines temperature as a physical quantity characterizing the mean random motion of molecules in a physical object(IAEA, 2008). Temperature can also be defined as a measure of how much warm or cold an object is. In general, temperature affects both living and non-living things in any ecosystem. For example, in the soil and soil ecosystem(Zuk-Golaszewska et al., 2003) temperature affects photosynthesis(Arai-Sanoh et al., 2010; Cai and Dang, 2002; Shah and Paulsen, 2003), respiration(WANG, 2004), transpiration (Boselli et al., 1998; Cox and Boersma, 1967; Clements and Martin, 1931; Gardner and Ehlig, 1963; Pallas et al., 1967), the water potential of the soil(Caron and Boudreau, 2006; Jong and Best 1979) soil translocation(Ge et al. 2015; Luan et al. 2014; Onwuka 2018; Trust and Phytologist, 2012), and microbial activities(Davidson and Janssens, 2006; Mew, 1977). Hence, it reduces crop product in terms of quantity and quality in agriculture(Valente et al. 2006). Generally, it is therefore affects the physio-chemical processes that are taken place on the earth.

Figure 1 depicts the different types of temperature measuring devices for different applications. The details of most of these devices are available in the originals works somewhere (Kedzierski, 1993; Fluke Corporation, 2006; Klaus-Dieter Gruner, 2003;Almaw Ayele Aniley et al., 2017;Naveen Kumar S K et al., 2019) but in this paper only thermistors is going to be explained because of their own advantages over the others.

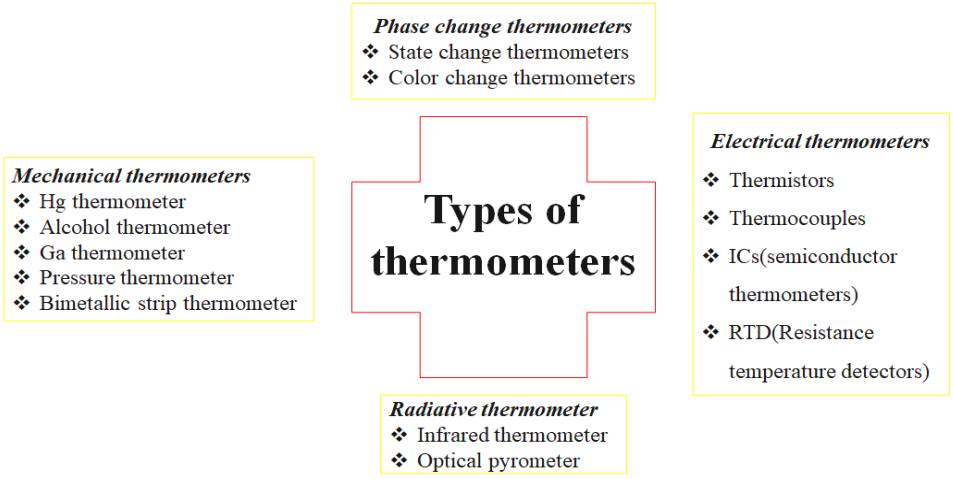

Figure 1. Classification of the available thermometers

The word thermistor is obtained from the two words thermal and resistor as a *Therm*ally sensitive res*istor*(Jacob Fraden, 2004; Jagtap et al., 2010). Based on the resistance temperature characteristics, thermistors can be classified as positive temperature coefficient resistance (PTCR) thermistors and negative temperature coefficient resistance (NTCR) thermistors. In PTCR thermistors as the temperature increases, the resistance also increases but in the case of NTC thermistors the opposite event occurs. The first evidence for the NTCR behaviour was registered on 21 February 1833, by the English philosopher Michael Faraday, who observed the resistance of silver sulphide, Ag_2S, to decrease with increasing temperature(Jacob Fraden,

2010). Thermistors can also be classified as low temperature (-323-423K) and high temperature (423-1173K) thermistors depending on the range of temperature they can measure. Low-temperature thermistors can be synthesized from mixed oxides of Mn, Ni, and Co. The principal advantages of using thermistors in measuring temperatures are having a large change of resistance with temperature i.e.,10 times higher than that of metals; availability in a wide range of resistances; no need of reference junction; little affected by the usual chemical and physical conditions of the environment(can be fully secured); small and mechanically rugged.

Thermistors can be fabricated as pellets, discs, rods and thick films. For example, Jungho Ryu et al fabricated NTC thermistor thick films of $NiMn_2O_4$ on the glass substrate by Aerosol Deposition (AD) at Room Temperature (RT)(Fluke Corporation, 2006). One big disadvantage of thick film thermistors is the presence of lead(Pb) as an adhesive material which is extremely toxic for life(Jagtap et al. 2010). In addition film fabrication techniques are complex and expensive.

In this work, synthesis and characterization of $NiMn_2O_4$ nanoceramic powder based and lead (Pb) free digital electronic thermometer probe fabrication, calibration and testing are discussed using simple and an economical method.

Thermistors are being used for many different areas of applications in every day to day activities of the society. To mention a few they used as temperature sensors, inrush current limiters, self-resetting over-current protectors and self-regulating heating elements etc.

2. Materials and Methods

There are two models for NTC thermistors (Gregg Lavenuta, 2018) namely the Stein and Hart model and the β-coefficient models. These models are given in equation (1) and equation (2) respectively.

$$\frac{1}{T(K)} = A + B.ln(R) + C.(ln(R))^3 \quad \text{Equ…1}$$

$$\frac{1}{T(K)} = \frac{1}{T_o(K)} + \frac{1}{\beta} ln(\frac{R}{R_o}) \quad \text{Equ…2}$$

Where, $T(k)$ is the temperature in degree Kelvin:A, B, and C are constants; R is the resistance of the thermistor in Ω; $T_o(K)$ is reference temperature; R_o is the resistance of the thermistor at reference temperature. The constants can be obtained simultaneously from any three temperature and resistance measurement data of the given thermistor. There are software to calculate the coefficients by providing the three resistance of the thermistor and the corresponding temperatures(Coefficient and Rt, 2012), for example, srs thermistor calculator. It is also very simple to calculate the coefficients and the constants using paper and pencil method. A simple Matlab code could also be written to solve any simultaneous equations in general.

From equation (2) β can be simplified and given in equation (3) to calculate β.

$$\beta = \frac{ln(\frac{R}{R_o})}{\frac{1}{T(K)} - \frac{1}{T_o(K)}} \quad \text{Equ…3}$$

2.1. Methods

2.1.1. Synthesise of $Nimn_2o_4$ Nanoceramic thermistor powder

The $NiMn_2O_4$ nanoceramic powder is synthesized by a modified wet chemical method called solution route. The 0.002 Kgms of tetra-hydrated Nickel acetate and 0.00394 Kgms of tetra-hydrated Manganese acetate powders are dissolved in 0.02 l of distilled water each in separate beakers. Each solution is kept in a magnetic stirrer on a hot plate at a temperature of 310K for 1800 seconds. Then after mix the two solutions and keep in a hot plate for 1800 more seconds. In addition, 0.0007 Kgms of Oxalic acid is dissolved in 0.0l l of distilled water in a separate beaker at room temperature. This solution is added to the previous solution under vigorous stirring condition that facilitates the chemical reaction and gel formation process. Then stirring is stopped and the resulting solution is kept at 343K on a hotplate until very thick sol is found. Next, this thick sol is dried in a muffle furnace at 373K for some time. Finally, the resulting powder is grounded using pestle and mortar and is calcined in a muffle furnace at 1223K for 12600-14400 seconds. The synthesis setup the resulting sample powder and the calcination process are shown in Figure 1(a, b & c) respectively.

Figure 1. Experimental setup (a), sample powder (b) and calcination(c)

FeSEM/EDS and powder XRD are used to characterize the surface morphology and average crystallite size, composition, and crystal structure of the resulting nanoceramic powder respectively.

2.1.2. Fabrication and calibration of the thermistor

The materials used and the detailed thermistor fabrication processes are shown stepwise in Figure 3. The characterization and the calibration setup is also shown in Figure 3. For characterization and calibration, we have used LM35 temperature sensor self interfaced with Atmega328 microprocessor-based microcontroller, homemade FTO coated glass heater, digital multimeter and computer loaded with the required software. The calibration experiment is conducted to relate the resistance and the temperature of the resulting thermistor. The experimental results are used for calculating thermistor based thermometer modelling parameters. We have used the two thermistor modelling techniques namely the Stein and Hart and the β-coefficient models. The thermistor modelling parameters are coefficients (A, B and C), the room temperature resistance (R_0), the room temperature (T_0) and β-coefficient or material constant.

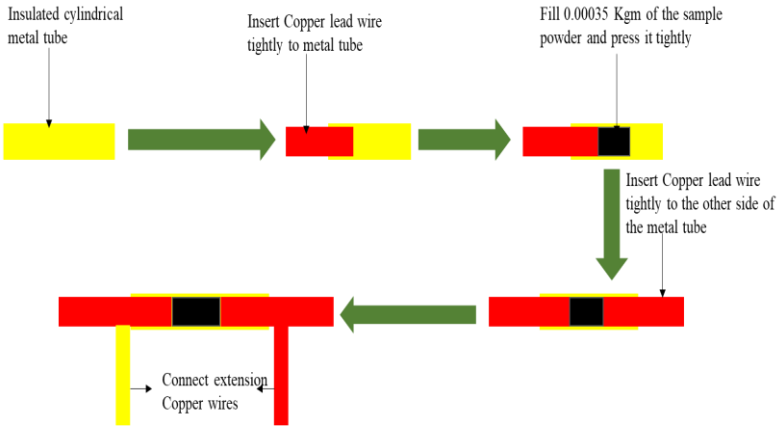

Figure 2. Fabrication process of the thermistor

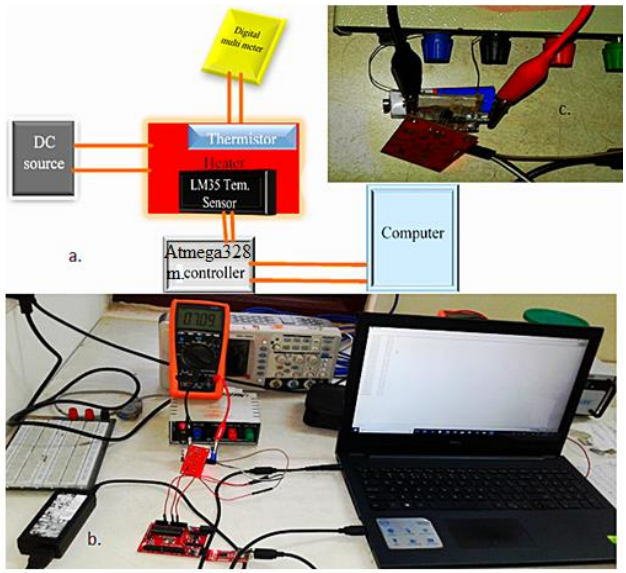

Figure 3. Characterization and calibration setup for the thermistor (a, in block diagram; b, physical characterization setup; c, component interconnection)

3. Results and Discussion

3.1. $NIMN_2O_4$ nanoceramic thermistor powder

The calcined powder is characterized using FeSEM/EDS for its morphology and particle size and composition respectively. The FeSEM result shows that the crystalline morphology of the ceramic powder and the size as shown in Figure 4b whereas, the EDS result confirms that the powder contains Ni, Mn, and O_2 in appropriate proportion as shown in Figure 4a.

The X-ray powder diffraction (XRPD) analysis was conducted in a Rigaku X-ray diffractometer using Bragg–Brentano geometry in the continuous mode with speed of 0.00883/second. Cu Ka radiation is used and the tube operated at 40000V and 0.025A current. The X-ray diffraction patterns are taken in the range of 10–80º in order to cover the most intense peaks of the $NiMn_2O_4$ phase. The crystallite size of the powder is determined using the Scherrer formula as given in equation (4).

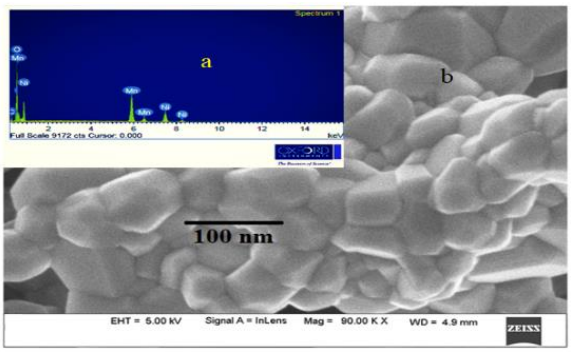

Figure 4. FeSEM/EDS characterization Result of the sample (a, EDS result; b, FeSEM result)

$$D = \frac{0.9\lambda}{\beta\cos(\theta)} \qquad \text{Equ…4}$$

Where λ is the x-ray wavelength of CuKα source 0.154059×10^{-9}m, θ is the Bragg's angle and β is the full width at half maximum (FWHM) of the diffraction peak in radians.

The average crystallite size of the nine peaks becomes about 34×10^{-9}m whereas, the minimum size is about 29×10^{-9}m which was observed at the seventh peak and the maximum size is about 38×10^{-9}m and observed in the first peak as shown in Figure 5. These results are also consistency within the range of the previous work(Almeida et al., 2008). The XRD result also confirms the existence of a spinel structure of the resulting nanoceramic powder.

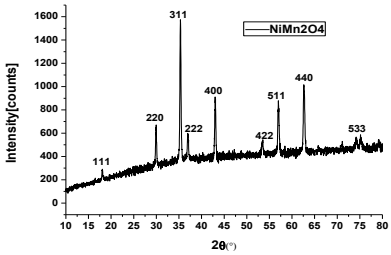

Figure 5. XRD result of the sample powder

3.2.Thermistor calibration results

The Stein and Hart and the β-coefficient models have been analysed and given in equations (5) and (6) respectively.

$$1/_{T(K)} = -0.006489926 + 0.0010145764\ln(R) - 0.000001598861(\ln(R))^3 \qquad \text{Equ…5}$$

Where $A = -0.006489926$, $B = 0.0010145764$ and $C = -0.00000159886$. The coefficients were calculated using the Matlab and srs software.

$$I/_{T(K)} = I/_{298.15K} + 1/_{6332.36K}\ln(\frac{R}{123.3646K\Omega}) \qquad \text{Equ…6}$$

Where $R_0 = 1233646\Omega$, $\beta = 6332.36K$ and $T_0 = 298.15K$. The two thermistor models are compared and they are compatible. Therefore, the mathematical models are representative of the practically measured thermistor characteristics.

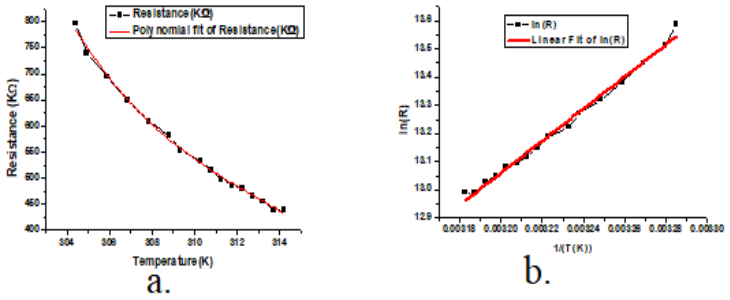

Figure 6.Ttemperature versus resistance characterization and calibration results of the thermistor (a, polynomial fit; b, linear fit)

Figure 6a shows the existence of a very good fit between third order polynomial and the resulting tested values of the thermistor. Figure 6b also confirmed the existence of a good linear fit of the thermistor model which assured the same. Therefore, the mathematical models are representative of the practically measured thermistor characteristics. This thermometer is used to measure the temperature up to 70 ℃.

3.3. Embedded system development results

The embedded system consists of both hardware and software. The hardware design is shown in Figure 7 in block diagram while the algorithm for the software design is shown in Figure 9 in the flow chart.

The fabricated thermistor, Atmega328, stainless steel tube, 16X2 LCD display, and 8cmx8cmx4cm 3-D printed plastic box for packaging, and 5V DC power supply hardware incorporated with Arduino programming software are used for the embedded system development. The 15cm long, 7mm inner diameter and 8mm outer diameter stainless steel tube is used as a probe (Figure 11) to hold thermistor. Stainless steel tube has two main functions namely protecting the sensor from rust and other damages, and easily inserted during installation and testing in the field.

Since the microcontrollers cannot read resistance and temperature directly, the resistance should be converted in the form of microcontroller readable physical quantities i.e., current or voltage signals. Therefore, the thermistor resistance variation should be converted into a voltage signal. To do so, a 1.02MΩ resistor is connected in series with the thermistor as a voltage divider. The detailed circuitry for the prototype of the system is shown in Figure 10. The complete circuit for the thermistor is shown in Figure 8. The voltage V_o is supplied to the microcontroller's one of the analogue terminals is given in equation(7)(web-1).

$$V_o = \frac{V_2 . R_{thermistor}}{R_{thermistor} + R} \qquad \text{(Equ…7}$$

The microcontroller displays a value which is given by the following formula (equation (8)):

$$ADC = \frac{1023 V_o}{V_{ref}} \qquad \text{(Equa…8}$$

If we substitute V_o from equation (7), we will get the following expression (equation (9)).

$$ADC = 1023 \left(\frac{V_2 . R_{thermistor}}{R_{thermistor} + R} \right) / V_{ref} \qquad \text{Equ…9}$$

If V_{ref}=V_2=5V, then equation (9) becomes (equation (10)):

$$ADC = 1023\frac{R_{thermistor}}{R_{thermistor} + R} \qquad \text{Equ…10}$$

From equation (10), $R_{thermistor}$ becomes (equation (11)):

$$R_{thermistor} = \frac{R}{(\frac{1023}{ADC} - 1)} \qquad \text{Equ…11}$$

$R_{thermistor}$, was substituted in the thermistor models to calculate the temperature. The final output of the microcontroller is temperature. The temperature is displayed on the 16X2 LCD display or serial monitor of the computer. The assembled and embedded system is shown in Figure 12. The algorithm for the software part of the system is shown in Figure 9 in flowchart.

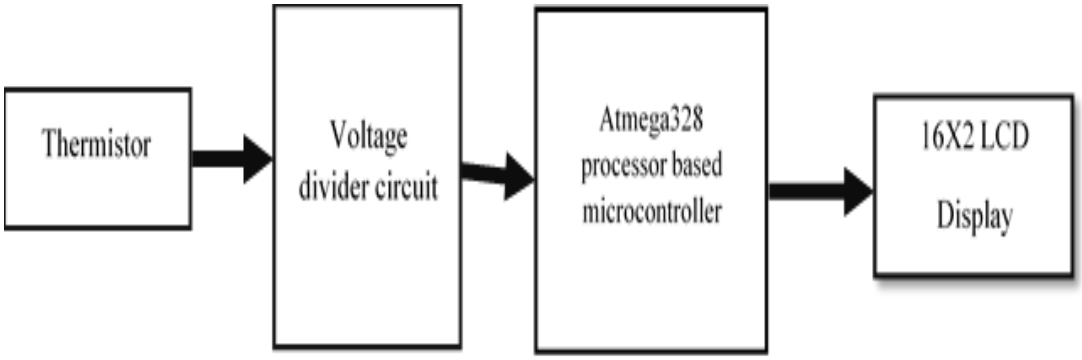

Figure 7. Design of the embedded system in block diagram

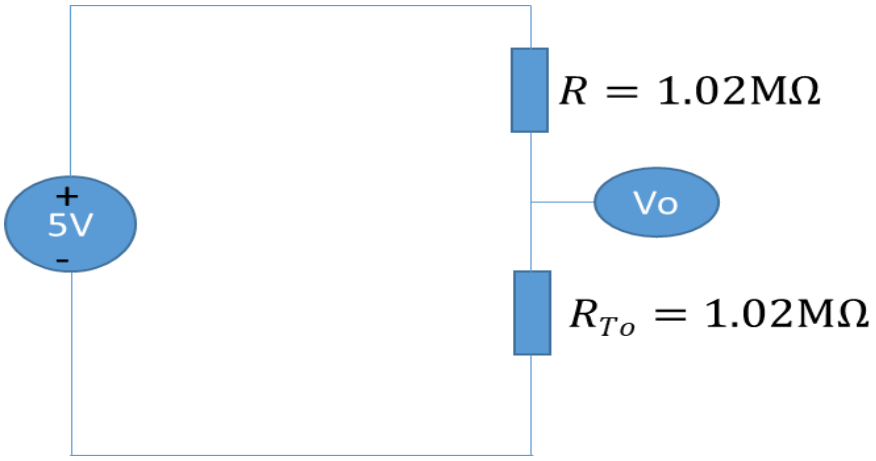

Figure 8. Voltage divider circuit for the microcontroller input

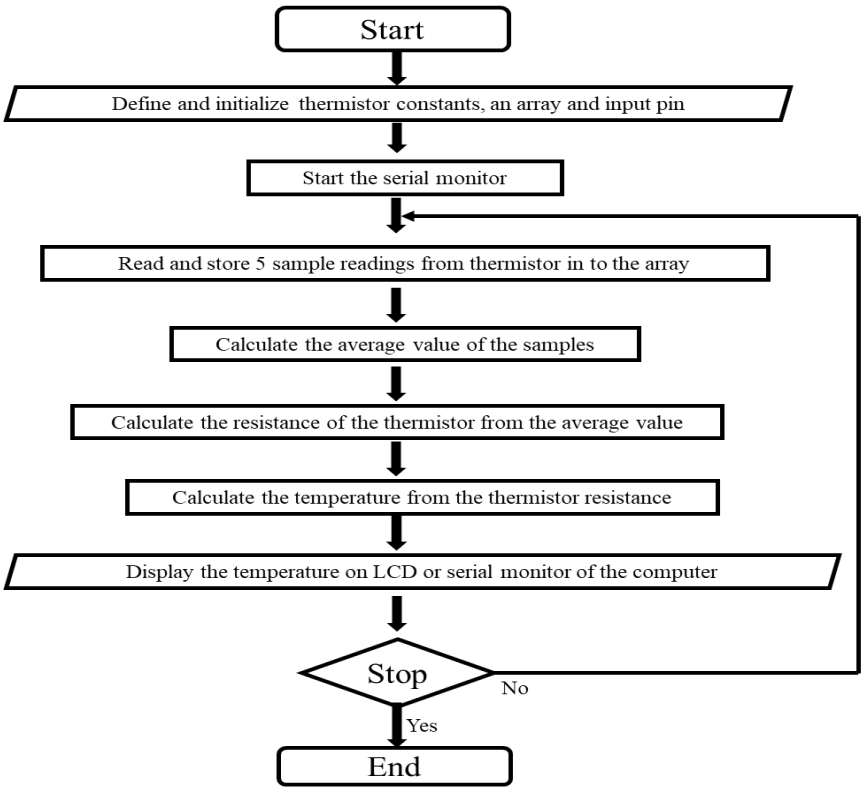

Figure 9. Design of the software part of the embedded system in the flowchart

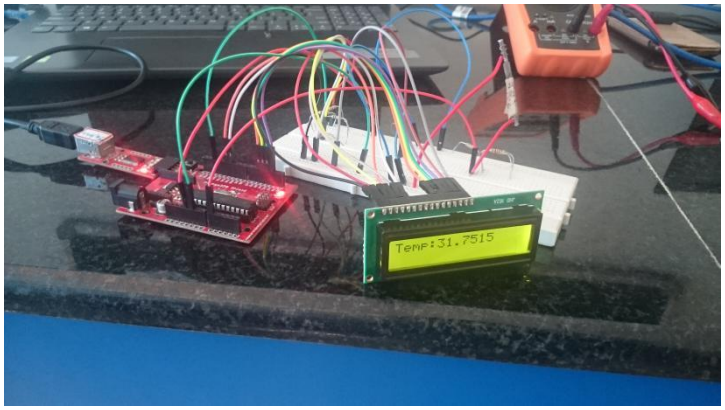

Figure 10. prototype of the embedded system

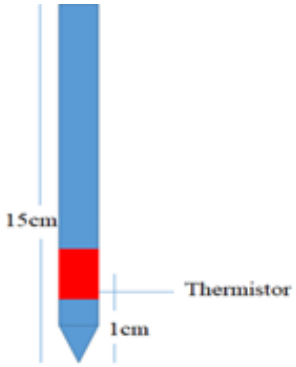

Figure 11. Designed thermometer probe

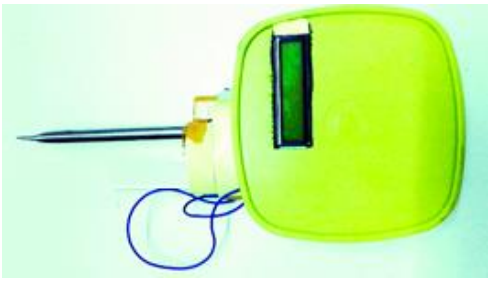

Figure 12. Fabricated embedded system

3.4.Testing the Thermometer

The fabricated thermometer has been tested by taking soil samples by adding water at different temperature as shown in Figure 13. LM35 IC temperature sensor and the fabricated thermometer are compared to measure the environment temperature. The readings are almost the same except small variation after the decimal point of the reading that is the maximum error read from the results is 0.033K. The result shows that the fabricated thermometer is working properly and the most promising especially in terms of cheap in cost, easy to prepare, easy to operate, durability and accuracy.

Figure 13. Application of the fabricated thermometer in real-time soil temperature monitoring in agriculture

4. Conclusion

Thermometer from NTC nanoceramic thermistor powders is prepared easily using an inexpensive method and simple procedure. The procedures are synthesizing nanoceramic powders, characterizing the powders, prepare the thermistor, characterize and calibrate the thermistor, develop the embedded system and finally test the thermometer. The unique features of this thermometer are up to four digit precision temperature measurement and does not require any pellet making or film-making process. The other advantage of this device is it is lead-free which is poison chemical. In the future, this thermometer can be modified and used for several other applications. For example for medical application, ambient temperature measurement application and other critical temperature measurement application areas.

Acknowledgements

The authors wish to acknowledge the University Grant Commission (UGC) for the partial financial support sponsored under the Indo-US Bilateral Research project.

Funding

No Funding has been received.

Competing Interests

The authors declare no competing interests.

Concerns to Publish

All the authors concern to the publication of this article.

References

Almaw Ayele Aniley, Naveen Kumar S.K, and Akshaya Kumar A. (2017). Soil Temperature Sensors in Agriculture and the Role of Nanomaterials in Temperature Sensors Preparation. IJEMS 7(2): 363–72. www.ijaert.org/wp-content/uploads/2018/01/131469.

Almaw Ayele Aniley Naveen Kumar S K Akshaya Kumar A Renny Edwin Fernandez, Shekhar Bhansali. (2019). Thin Film Dual Probe Heat Pulse (DPHP) Micro Heater Network for Soil Moisture Content Estimation in Smart Agriculture. Journal of The Electrochemical Society 166(2): B63–67. http://jes.ecsdl.org/lookup/doi/10.1149/2.0511902jes.

Almaw Ayele Aniley Naveen Kumar S K Akshaya Kumar A Renny Edwin Fernandez, Shekhar Bhansali. (2019). Fabrication, Characterization and Comparison of Nanocrystalline NiMn2O4 and NiZn0.2Mn1.8O4 NTCR Ceramic Thermistor Powders. Journal of Nanoscience and Technology 5(1): 603–606.

Almeida, J M A et al. (2008). Synthesis and Characterization of NiMn 2 O 4 Nanoparticles Using Gelatin as Organic Precursor. Journal of Magnetism and Magnetic Materials 320: 304–7.

Arai-Sanoh, Yumiko, Tsutomu Ishimaru, Akihiro Ohsumi, and Motohiko Kondo. (2010). Effects of Soil Temperature on Growth and Root Function in Rice. Plant Production Science 13(3): 235–42. https://www.tandfonline.com/doi/full/10.1626/pps.13.235.

Boselli, Maurizio, Claudio Di Vaio, and Brunella Pica. (1998). Effect of Soil Moisture and Transpiration on Mineral Content in Leaves and Berries of Cabernet Sauvignon Grapevine. Journal of Plant Nutrition 21(6): 1163–78.

Cai, T, and Q L Dang. (2002). Effects of Soil Temperature on Parameters of a Coupled Photosynthesis-Stomatal Conductance Model. Tree physiology 22(12): 819–28. http://treephys.oxfordjournals.org/cgi/doi/10.1093/treephys/22.12.819%5Cnpapers2://publication/doi/10.1093/treephys/22.12.819.

Caron, Jean, and Jocelyn Boudreau. (2006). Soil Water Potential Detector. (May): 6.

Coefficient, Negative Temperature, and Where Rt. (2012). Calibrate Steinhart-Hart Coefficients for Thermistors. (408): 1–3.

Cox, L M, and L Boersma. (1967). Transpiration as a Function of Soil Temperature and Soil Water Stress. Plant physiology 42(4): 550–56. http://www.pubmedcentral.nih.gov/articlerender.fcgi?artid=1086580&tool=pmcentrez&rendertype=abstract.

David, Nathan, Abafor Chima, Aronu Ugochukwu, and Edoga Obinna. (2015). Design-of-a-Home-Automation-System-Using-Arduino.Docx.

Davidson, Eric A., and Ivan A. Janssens. (2006). Review: Temperature Sensitivity of Soil Carbon Decomposition and Feedbacks to Climate Change. Nature 440: 165–73.

F. E. Clements and E. V. Martin. (1931). Effect of soil temperature on transpiration in helianthus annuus. clements and martin: Soil temperature and transpiration (2): 619–30.

Fluke Corporation. (2006). Infrared Thermometer User Manual. Science (New York, N.Y.): 483. http://www.ncbi.nlm.nih.gov/pubmed/17781896.

Gardner, W. R., and C. F. Ehlig. 1963. "The Influence of Soil Water on Transpiration by Plants." Journal of Geophysical Research 68(20): 5719–24. http://doi.wiley.com/10.1029/JZ068i020p05719.

Ge, Liqiang, Long Cang, Hui Liu, and Dongmei Zhou. (2015). Effects of Different Warming Patterns on the Translocations of Cadmium and Copper in a Soil–Rice Seedling System. Environmental Science and Pollution Research 22(20): 15835–43.

Goswami, Rishikesh, and Rakesh Kumar. (2018). Design Fabrication and Satic Calibration of Thermocouple and Thin Film Gauges. IOP Conference Series: Materials Science and Engineering 377(1).

Gregg Lavenuta. (2018). An explanation of the beta and steinhart-hart equations for representing the resistance vs. temperature relationship in ntc thermistor materials. QTI Sensing Solutions.

Hamed, Basil, and Basil Hamed. (2015). Design & Implementation of Smart House Control Using LabVIEW Design & Implementation of Smart House Control Using LabVIEW.

Husain, Muhammad Dawood, Richard Kennon, and Tilak Dias. (2014). Design and Fabrication of Temperature Sensing Fabric. Journal of Industrial Textiles 44(3): 398–417.

IAEA. (2008). Atomic Energy Field Estimation of Soil Water Content: A Practical Guide to Methods, Instrumentation and Sensor Technology. Vienna.

Jacob Fraden. 2004. Handbook of Modern Sensors:PHYSICS, DESIGNS, and APPLICATIONS. 3rd ed. Calfornia: Springer.

Jacob Fraden.(2010). Handbook of Modern Sensors:Physics, Designs, and Applications. 4th ed. London: Springer.

Jagtap, Shweta, Sunit Rane, Suresh Gosavi, and Dinesh Amalnerkar. (2010). Low Temperature Synthesis and Characterization of NTC Powder and Its 'lead Free' Thick Film Thermistors. Microelectronic Engineering 87(2): 104–7. http://dx.doi.org/10.1016/j.mee.2009.05.026.

Kedzierski, Mark a. 1993. "Principles and Methods of Temperature Measurement." Experimental Thermal and Fluid Science 6(1): 106.

Klaus-Dieter Gruner. (2003). Principles of Non-Contact Temperature Measurement. Raytek Corporation. www.raytek.com.

Luan, Junwei et al. (2014). Different Effects of Warming and Cooling on the Decomposition of Soil Organic Matter in Warm–Temperate Oak Forests: A Reciprocal Translocation Experiment. Biogeochemistry 121(3): 551–64.

Mew, T. W. (1977). Effect of Soil Temperature on Resistance of Tomato Cultivars to Bacterial Wilt. Phytopathology 77: 909.

Naveen Kumar S K, Akshaya Kumar A, Almaw Ayele Aniley, Renny Edwin Fernandez, and Shekhar Bhansali. (2019). Hydrothermal Growth of Zinc Oxide (ZnO) Nanorods (NRs), Structural, and Chemical Composition Studies for PH Measurement Sensor Applications Naveen Kumar S K. In ECS Transactions,88, 437–47.

Naveen Kumar S K, Almaw Ayele Aniley, Akshaya Kumar A, Renny Edwin Fernandez, Shekhar Bhansali. (2019). Nanoceramic NiMn 2 O 4 Powder-Based Resistance

Thermometer for Soil Temperature Measurement Application in Agriculture Naveen Kumar S.K. In ECS Transactions,88 , 455–70.

Onwuka, Brownmang. (2018). Effects of Soil Temperature on Some Soil Properties and Plant Growth. Advances in Plants & Agriculture Research 8(1).

Ota, Hiroki et al. (2017). 3D Printed 'Earable' Smart Devices for Real-Time Detection of Core Body Temperature. ACS Sensors 2(7): 990–97.

Pallas, J E, B E Michel, D G Harris, and D. G. Harris. (1967). Photosynthesis, Transpiration, Leaf Temperature, and Stomatal Activity of Cotton Plants under Varying Water Potentials. Plant physiology 42(1): 76–88.

Priyadarshi, Aditya. (2015). Design and Fabrication of Plate Thermometer for the Measurement of Incident Radiation Heat Flux on a Surface. International Journal of Science and Research (IJSR) 4(8): 1460–65.

R. DE JONG and K. F. BEST. (1979). The Effect of Soil Water Potential, Temperature and Seeding Depth on Seedling Emergence of Wheat. Can. J. Soll Sci. 59: 259–64.

Reza, Md. Selim, SM Mamun, and Munna Monjur Mossadded. (2018). Design and Development of a GSM-Based Smart Home Automation System: A Low Cost Approach. Preprints (November): 1–5.

Sahu, S et al. (2015). Design and Fabrication of a Data Logger for Atmospheric Pressure, Temperature and Relative Humidity for Gas-Filled Detector Development.

Shah, N. H., and G. M. Paulsen. (2003). Interaction of Drought and High Temperature on Photosynthesis and Grain-Filling of Wheat. Plant and Soil 257(1): 219–26.

Sun, Yiwei et al. (2018). Fabrication of Composite Microneedle Array Electrode for Temperature and Bio-Signal Monitoring. Sensors 18(4): 1–12.

Trust, New Phytologist, and New Phytologist. (2012). Effect of Temperature on Wood Decay and Translocation of Soil-Derived Phosphorus in Mycelial Cord Systems. New Phytologist 129(2): 289–97. http://doi.wiley.com/10.1111/j.1469-8137.1995.tb04299.x.

Valente, A. et al. (2006). Multi-Functional Probe for Small-Scale Simultaneous Measurements of Soil Thermal Properties, Water Content, and Electrical Conductivity. Sensors and Actuators, A: Physical 132: 70–77.

WANG, Gengchen. (2004). Experimental Study on Soil Respiration of Temperate Grassland in China. Chinese Science Bulletin 49(6): 642. http://www.scichina.com/2004/ky/0406/ky0642.stm.

Web-1: Https://Learn.Adafruit.Com/Thermistor/Using-a-Thermistor, consulted 5 September 2019.

Zuk-Golaszewska, Krystyna, M. K. Upadhyaya, and J. Golaszewski. (2003). The Effect of UV-B Radiation on Plant Growth and Development. Plant, Soil and Environment 49(3): 135–40.